Electron Lenses and Computational Methods

Luke Horgan

1 Abstract

In the 17th century, the first microscopes brought the world into clearer focus. Dutch scientist Antonine van Leeuwenhoek, widely considered the father of microbiology, famously used them to discover that living tissue is composed of cells. The resolution of conventional microscopes, however, is severely constricted by the wavelength of visible light. It is possible to sidestep this issue somewhat by using special ultraviolet microscopes, but for extremely high magnifications, electron microscopy becomes necessary. Electron lenses work by focusing a beam of electrons onto a small area, just as the optical lenses in a conventional microscope work by focusing light. However, they accomplish this by means of a carefully calibrated magnetic field. In this paper, we examine the principles of operation of electron lenses, and we develop analytical methods for simulation of some of their properties.

2 Motivation

Electron microscopes work by focusing a beam of electrons, emitted thermionically [3] from a heated cathode, onto a specimen. In a transmission electron microscope, the image signal is generated from electrons in the beam which manage to pass through the sample, which must be very thin [7]. In a scanning electron microscope, the image signal consists primarily of backscattered electrons, which are emitted from the specimen when the high-energy beam strikes it. Both microscopes use a series of electrostatic and magnetic lenses to focus the electron beam. Scanning electron microscopes also use magnetism to deflect the electron beam in carefully controlled increments, so that the image can be generated pixel by pixel as the beam sweeps over the specimen [8].

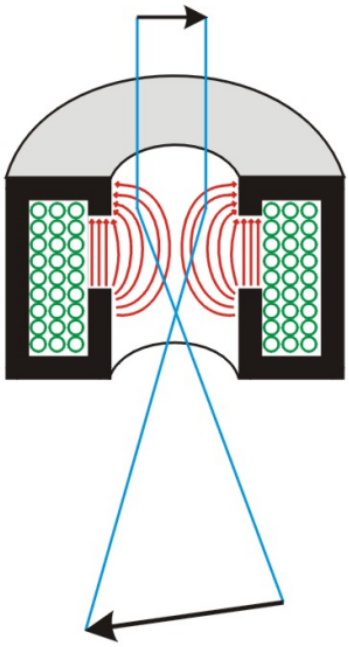

Figure 1: An electron lens, featuring copper coils (green) surrounded by an iron pole-piece [5]

We focus exclusively on the magnetic lenses, which are the bread and butter of any self-respecting electron microscope.

3 Mathematical Background

An electron lens consists of multiple coils of copper wire surrounded, apart from an open slit, by an iron sheath called a pole piece. A current passing through the coils produces a magnetic field, which is concentrated by the pole piece. [7]

Electrons passing through the lens will be focused at a point known as the crossover, and then they will once more diverge before encountering the specimen to be imaged. A commercial microscope will typically feature at least two magnetic electron lenses and one electrostatic lens, called a Wenhelt cylinder [2]. The particulars of optics and image formation are beyond the scope of this paper. Our purpose here is to motivate the development of a computer model for electron trajectories in a magnetic lens by developing a common model for their motion and highlighting its shortcomings.

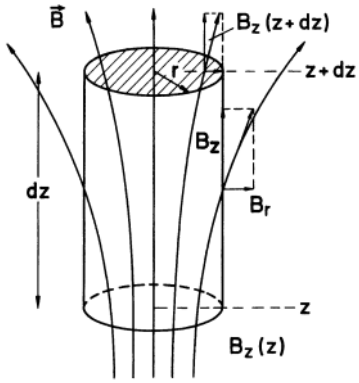

Figure 2: Magnetic flux through a small cylinder of radius r and height dz [7]

.

Reimer does this using the well-known Glockenfeld distribution (German for bell field). We will walk through Reimers derivation, following the general structure and filling in the bits that are, in our opinion, somewhat unclear.

$$B_z = \frac{B_0}{1 + (\frac{z}{a})^2} \tag{1}$$

Here $2a$, is the maximum field strength in the center of the lens and is the full width at half maximum, as indicated in Fig 1. But what of the other components? The lens geometry clearly yields rotational symmetry, so we need only derive an expression for the rotational component, which we can do by invoking Maxwells equations. In particular:

$$\nabla \cdot \vec{B} = 0 \tag{2}$$

Consider the cylinder of Figure 2. Let us calculate the flux through each surface of the cylinder:

$$\pi r^2 B_z(z) \tag{3}$$

$$\pi r^2 B_z(z + dz) \tag{4}$$

$$2\pi B_r dz \tag{5}$$

Equations 2, 3, and 4 treat the flux through the bottom, top, and sides of the cylinder, respectively. The divergence of the magnetic field, then, is:

$$\nabla \cdot \vec{B} = \pi r^2 B_z(z) - \pi r^2 B_z(z+dz) - 2\pi B_r dz = 0 \tag{6}$$

Solving for B_r, we obtain:

$$B_r = \frac{rB_z(z)}{2dz} - \frac{rB_z(z+dz)}{2dz} \tag{7}$$

Expanding $B_z(z+dz)$ as $B_z + (\frac{\delta B_z}{\delta z})dz + ...$, we arrive at:

$$B_r \approx \frac{r}{2}\frac{\delta B_z}{\delta z} \tag{8}$$

Now that we have the field, we need to understand the force it produces. In cylindrical coordinates, the acceleration vector is:

$$\vec{a} = (\ddot{r} - r\dot{\theta}^2)\hat{r} + (r\ddot{\theta} + 2\dot{r}\dot{\theta})\hat{\theta} + \ddot{z}\hat{z} \tag{9}$$

From this (and Newton's second law), it follows directly that:

$$F_r = m(r\dot{\theta}^2 - \ddot{r}) \tag{10}$$

$$F_z = m\ddot{z} \tag{11}$$

$$rF_\theta = mr(r\ddot{\theta} + 2\dot{r}\dot{\theta}) = \frac{d}{dt}(mr^2\dot{\theta}) \tag{12}$$

where is the mass of an electron.

Now, using the Lorentz force law $-e\vec{v}\times\vec{B}$ and substituting our definition of from above and , we find:

$$F_r = -er\dot{\theta}B_z \tag{13}$$

$$F_\theta = e\dot{r}B_z + e\dot{z}(\frac{r}{2}\frac{\delta B_z}{\delta z}) \tag{14}$$

$$F_z = er\dot{\theta}\frac{r}{2}\frac{\delta B_z}{\delta z} \tag{15}$$

Combining equations 10-12 and 13-15 and rearranging, we obtain:

$$m\ddot{r} = -eB_z r\dot{\theta} + mr\dot{\theta}^2 \tag{16}$$

$$\frac{d}{dt}(mr^2\dot{\theta}) = eB_z r\dot{r} + e\frac{r^2}{2}\dot{z}\frac{\delta B_z}{\delta z} = \frac{d}{dt}(\frac{e}{2}r^2 B_z) \tag{17}$$

$$m\ddot{z} = eB_r r\dot{\theta} \tag{18}$$

These equations completely describe the (approximate) motion of an electron passing through the glockenfeld. Reimer takes this a step further and produces a more convenient form in terms of potential energy, but this requires considerations of relativity which are beyond the scope of this paper.

This model is good for building an understanding of the working principle of an electron lens, but it is filled with assumptions, the most constraining of which is that the lens must have the very simple geometry of Fig 1 for these equations to apply.

4 The Computer Model

Our computer model offers the kernel of a solution to this problem by enabling the numerical approximation of the electric and magnetic fields and forces of arbitrarily complex geometries. The magnetic field of a volume current is given by the Biot-Savart law [4]:

$$\vec{B}(\vec{r}) = \frac{\mu_0}{4\pi} \int \frac{\vec{J}(\vec{r'}) \times \hat{\mathcal{R}}}{|\mathcal{R}|^2} d\tau' \tag{19}$$

Computation of this integral may be carried out using Monte Carlo integration [1]. That is, we randomly pick n points within the user-specified mesh and find the value of the integrand at each of those points. Then, we multiply by the volume of the mesh and divide by n.

There is one important complication, though; we may assume a uniform current within the volume of our geometry, but we cannot expect the user to specify which way it is flowing at every point. Our solution is to use the method of relaxation. Users hook their mesh to two virtual nodes, a source and a sink, and the current direction at every point in the mesh is then approximated by assuming current will be maximally flat and wont bunch up anywhere. The potential of any point falling within the volume of either node is fixed at a set value, the only necessity being that the source potential is higher than that of the sink. All points in between are initialized to have a potential of 0, and then they are successively updated with the average value of their nearest neighbors. This method gradually converges on a good approximation of the current direction at each point (even in very strange geometries!).

Note that we apply a slight optimization of the algorithm, as proposed by Mallinckrodt [6]. The idea is to anticipate future iterations by overcorrecting on each point. That is, instead of adding the difference of the points old value and the average value of its neighbors, $\Delta = \textit{old value} - \textit{new value}$, to

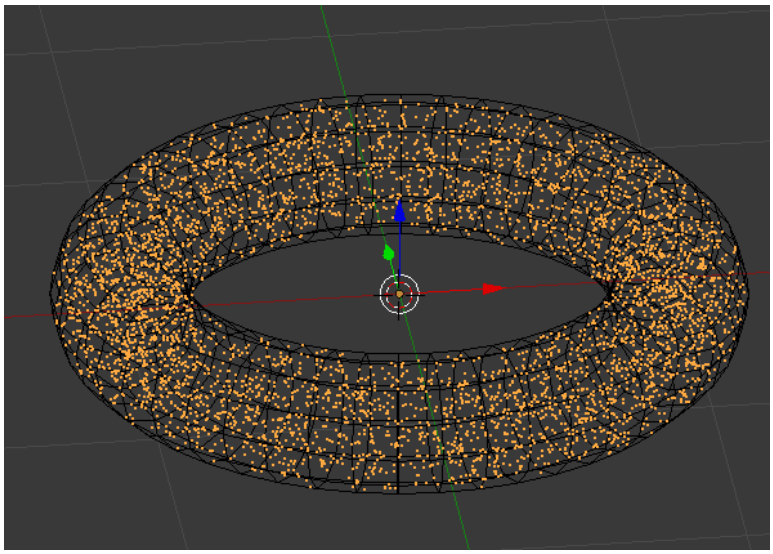

Figure 3: The stochastic donut. Or, more precisely, 5000 random points inside of a torus, highlighted in orange.

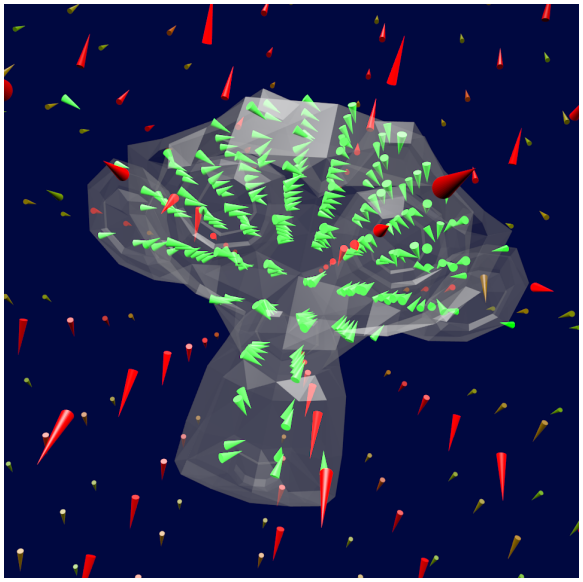

Figure 4: The green cones represent the current flowing through the head of Suzanne, the monkey mascot of Blender, which was used to render the image. The source/sink are connected between her ears, as can be seen in Figure 9.

its current value (which is effectively just replacing it by the average of its neighbors), we instead add $C\Delta$, where C is some constant greater than 1. We use 1.5.

The results of this method for some common geometries are shown in Figure 5.

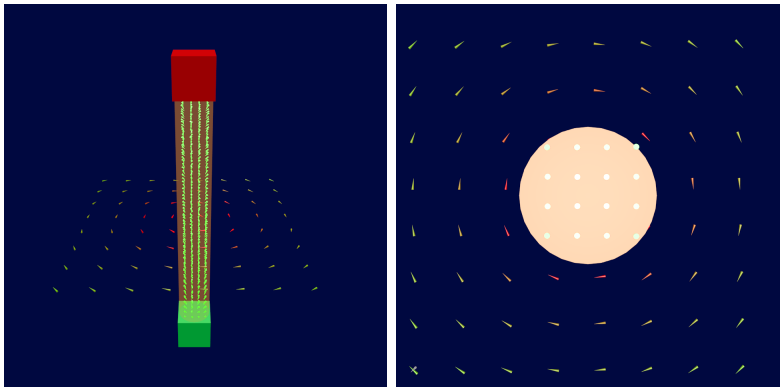

(a) Front view (b) Top view

Figure 5: The magnetic field of a current-carrying wire. The field is strongest where the cones are red, and weakest where they are green. In the image on the left, it is possible to see the automatically calculated current alignment.

The electric field may be calculated with an identical Monte Carlo methodology, using the relation [4]:

$$\vec{E}(\vec{r}) = \frac{1}{4\pi\epsilon_0}\int \frac{\rho(\vec{r'})}{\mathcal{R}^2}\hat{\mathcal{R}}d\tau' \tag{20}$$

This integration, however, is somewhat simpler to carry out, because the direction of $\hat{\mathcal{R}}$ is trivially calculated as $\frac{r'-r}{|r'-r|}$; there is no current direction to fiddle with. Note that we assume we are working with uniform charge distribution, so equation 20 may equivalently be written as:

$$\vec{E}(\vec{r}) = \frac{Q}{4\pi\epsilon_0}\int \frac{1}{\mathcal{R}^2}\hat{\mathcal{R}}d\tau' \tag{21}$$

Some canonical geometries are featured in Figure 7.

Note that for complex geometries involving multiple meshes, we can use superposition to calculate the overall electric and magnetic fields.

At last, we can also find the force on a charge q travelling at velocity $\vec{v}$ from:

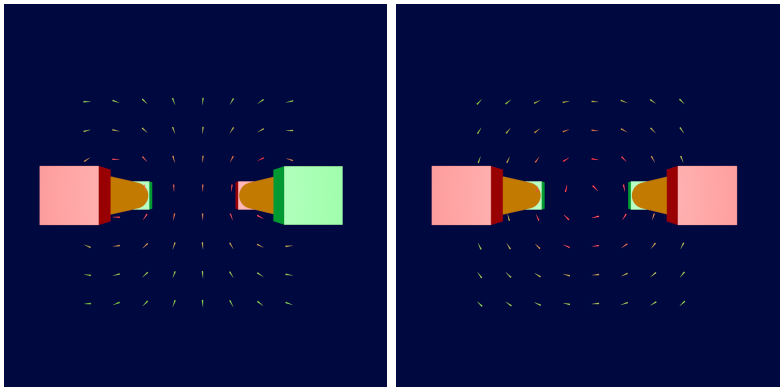

(a) Oppsoite currents (b) Same currents

Figure 6: Magnetic field surrounding two current-carrying wires. In the figure on the left, the currents are flowing in opposite directions. In the field on the right, they are moving in the same direction. Note that no code had to be changed to generate these two fields; only the green and red source/sink cubes had to be flipped.

$$\vec{F} = q\vec{E} + q\vec{v} \times \vec{B} \tag{22}$$

5 Next Steps

Of course, the whole point of simulating the magnetic/electric fields, and then the force, is to calculate the trajectories of the charged particles (electrons) travelling within them. Using our work as a starting point, this should be relatively straightforward. Indeed, the code on Github includes a method to do it, but it doesnt take relativity into account, so its rather useless for any practical purpose. The algorithm itself is simple, and the principle is the same whether relativity is accounted for or not. Assume the electron has initial velocity $\vec{v}$. Calculate the force acting on it at some start point $\vec{p}$. Use this to calculate its acceleration vector $\vec{a}$. Move it some small distance along δ, and calculate $\vec{p'}$ and $\vec{v'}$. Repeat this procedure as many times as desired to plot out the electrons course over some volume.

A more complicated shortcoming to address is that our models cannot presently simulate ferromagnetism, meaning that there is no way to simulate the iron shielding surrounding the scan coils. One workaround would be to model the sheathing as an electromagnet instead.

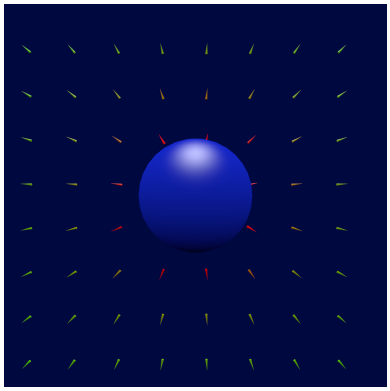

(a) Positively charged sphere

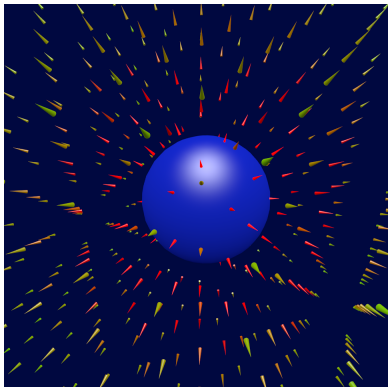

(b) A fun perspective

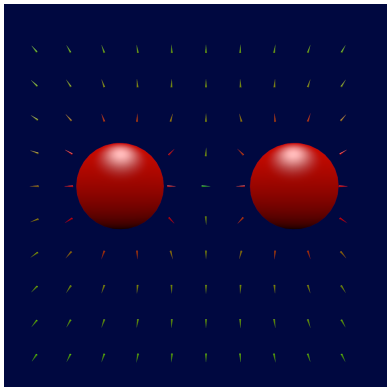

(c) Two identical spheres

Figure 7: The top images show the electric field surrounding a single positively charged sphere. The image on the right is a beauty shot highlighting how lovely these fields can look when visualized. The bottom image shows the field of two identical, uniformly charged spheres.

6 Conclusion

Electron microscopes are fantastically useful tools for peering into well-hidden details of the world around us, but conventional pen-and-paper models for electron motion are cumbersome and highly approximate. We have developed the basis of an extensible, flexible model for particle motion that uses only readily available open source software. Although many complete models certainly exist, ours does have the unique advantage of being completely free and also fairly easy to use. It may well prove useful, in a practical sense, once we include simulated particle trajectories. Certainly, we learned

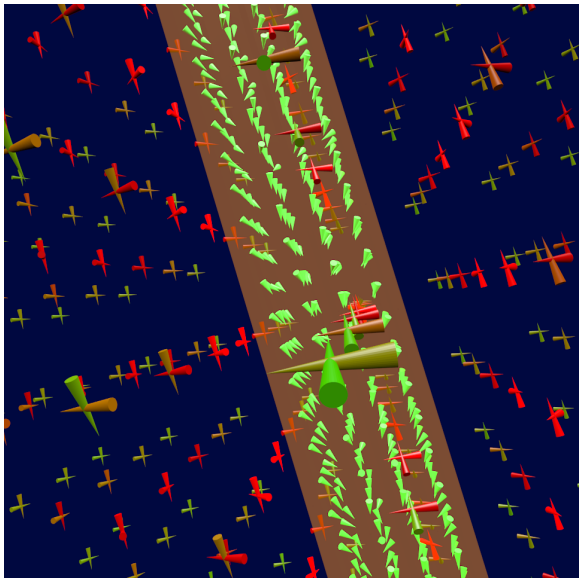

Figure 8: Here we see force vectors imposed on the magnetic field vectors of the current carrying wire from Figure 5, where the force is on a heavy charged particle moving at half the speed of light in the x direction.

a lot in developing it.

Code is available on GitHub at: `https://github.com/lhorgan/fieldsim`.

References

[1] Monte carlo integration.

[2] Wenhelt cylinder.

[3] Ral Baragiola. Thermionic emission, Sep 2000.

[4] David J Griffiths. *Introduction to Electrodynamics*. Pearson, 2015.

[5] F. Krumeich. Principle of an electromagnetic lens.

[6] A. J Mallinckrodt. Cylindrical coordinates.

[7] Ludwig Reimer. *Transmission Electron Microscopy*. Springer, 1997.

[8] Ludwig Reimer. *Scanning Electron Microscopy*. Springer, 1998.

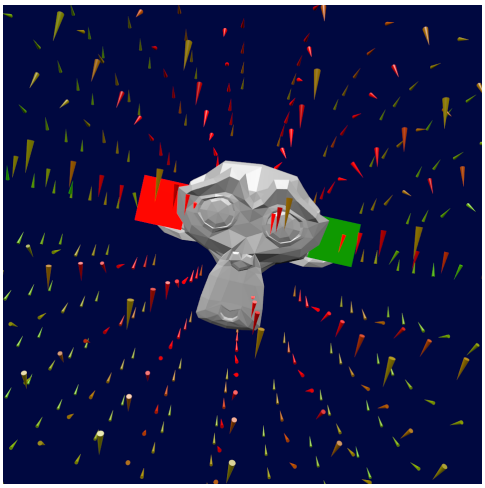

Figure 9: Just for fun. The magnetic field surrounding Suzanne. The pseudo-electrodes are connected between her ears (red anode, green cathode).